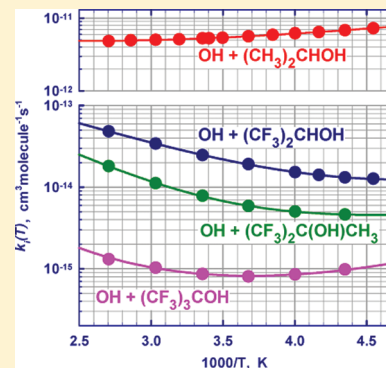


High Accuracy Measurements of OH Reaction Rate Constants and IR Absorption Spectra: Substituted 2-Propanols

Vladimir L. Orkin,^{*,†} Victor G. Khamaganov,[†] and Michael J. Kurylo[‡][†]National Institute of Standards and Technology, Gaithersburg, Maryland 20899, United States[‡]Goddard Earth Sciences, Technology, and Research (GESTAR) Program, Universities Space Research Association, Greenbelt, MD 20771, United States

Supporting Information

ABSTRACT: Rate constants for the gas phase reactions of OH radicals with 2-propanol and three fluorine substituted 2-propanols, (CH₃)₂CHOH (*k*₀), (CF₃)₂CHOH (*k*₁), (CF₃)₂C(OH)CH₃ (*k*₂), and (CF₃)₃COH (*k*₃), were measured using a flash photolysis resonance-fluorescence technique over the temperature range 220–370 K. The Arrhenius plots were found to exhibit noticeable curvature for all four reactions. The temperature dependences of the rate constants can be represented by the following expressions: *k*₀(*T*) = 1.46 × 10⁻¹¹ exp{-883/*T*} + 1.30 × 10⁻¹² exp{+371/*T*} cm³ molecule⁻¹ s⁻¹; *k*₁(*T*) = 1.19 × 10⁻¹² exp{-1207/*T*} + 7.85 × 10⁻¹⁶ exp{+502/*T*} cm³ molecule⁻¹ s⁻¹; *k*₂(*T*) = 1.68 × 10⁻¹² exp{-1718/*T*} + 7.32 × 10⁻¹⁶ exp{+371/*T*} cm³ molecule⁻¹ s⁻¹; *k*₃(*T*) = 3.0 × 10⁻²⁰ × (*T*/298)^{11.3} exp{+3060/*T*} cm³ molecule⁻¹ s⁻¹. The atmospheric lifetimes due to reactions with tropospheric OH were estimated to be 2.4 days and 1.9, 6.3, and 46 years, respectively. UV absorption cross sections were measured between 160 and 200 nm. The IR absorption cross sections of the three fluorinated compounds were measured between 450 and 1900 cm⁻¹, and their global warming potentials were estimated.



1. INTRODUCTION

The international phase-out of the production and use of ozone-destroying chemicals under the Montreal Protocol on Substances that Deplete the Ozone Layer and its subsequent Amendments and Adjustments has stimulated considerable research on the atmospheric properties of potential chemical substitutes.¹ Chlorine-free, partially fluorinated hydrocarbons (hydrofluorocarbons or HFCs) have been among the leading ozone-friendly substitutes for chlorofluorocarbons (CFCs) originally targeted under the Montreal Protocol. However, rising concern about the potential impact of various industrial halocarbons on the Earth's climate has stimulated further search for chemicals that satisfy various industrial needs while having little impact on either stratospheric ozone or climate.^{2,3}

Quantification of the possible role of new compounds as "greenhouse gases" requires accurate information on their atmospheric lifetimes, which are key parameters in determining the environmental consequences of their release into the atmosphere. These data, when combined with IR absorption spectra, allow estimations of radiative forcing and global warming potentials (GWPs) through either radiative-transfer modeling or semiempirical calculations. This search has been particularly focused on chemicals having very short residence times in the lower atmosphere as a result of either photolysis or reaction with the hydroxyl radical (OH). Significant photolytic loss is limited to chemicals containing bromine and iodine. Hence, the atmospheric lifetimes of most of the fluorine-containing chemicals being considered as replacements for

CFCs and halons are controlled in large part by their reactivities with tropospheric OH. On the other hand, the very-short-lived hydrogen-containing compounds can contribute to the ground-level ozone formation near to the emission locations depending on the local atmospheric chemical composition. The photochemical ozone creation potential (POCP), a well-established method of ranking compounds by their ability to form ozone in the troposphere,¹ also depends on the rate constant of the reaction between a compound and OH.⁴

Fluorinated alcohols are one such class of ozone-friendly chemicals being considered as CFC substitutes in certain industrial applications. These chemicals can be removed from the atmosphere by wet and dry deposition and by reaction with tropospheric OH, with the latter expected to be the most significant loss process. Hence, OH reaction rate constants for such compounds are required to determine their atmospheric lifetimes and possible effects on the Earth's radiation budget (i.e., their GWPs). While the nature and fate of the oxidation products from such reactions are also important in determining environmental acceptability, information on the initial rate of reaction is a necessary first step.

Special Issue: A. R. Ravishankara Festschrift

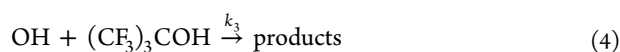
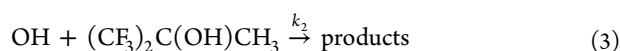
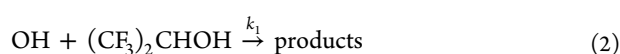
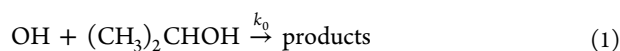
Received: November 30, 2011

Revised: February 24, 2012

Published: February 28, 2012

In our laboratory we have been focusing on precise and accurate measurements of the OH reaction rates of many naturally occurring and anthropogenic halocarbons. Such data are useful not only in the screening of new industrial chemicals for environmental acceptability, but also for estimating the reactivity (and lifetimes) of chemicals not yet in production using empirical correlations or more elaborate ab initio calculations. Recently, we reported the results of accurate studies of ethanol and its fluorinated substitutes, $\text{CH}_2\text{FCH}_2\text{OH}$, $\text{CHF}_2\text{CH}_2\text{OH}$, and $\text{CF}_3\text{CH}_2\text{OH}$.²⁴ Only the β -carbon (methyl group) can be fluorinated in the ethanol molecule whereas the main OH reaction channel is a H abstraction from α -carbon (methylene group). The α -carbon of ethanol can be fluorinated via trifluoromethyl group substitution, however.

This paper reports the results from our investigations of the reactions of the OH radical with 2-propanol and three substituted 2-propanols— $(\text{CF}_3)_2\text{CHOH}$ (1,1,1,3,3,3-hexafluoro-2-propanol), $(\text{CF}_3)_2\text{C}(\text{OH})\text{CH}_3$ (1,1,1,3,3,3-hexafluoro-2-methyl-2-propanol, hexafluoro-2-methylisopropanol), and $(\text{CF}_3)_3\text{COH}$ (1,1,1,3,3,3-hexafluoro-2-(trifluoromethyl)-2-propanol, perfluoro-tert-butanol):



They all can be considered as ethanol derivatives: 1-methylethyl alcohol, 2,2,2-trifluoro-1-(trifluoromethyl)-ethanol, 1,1-bis(trifluoromethyl)-ethanol, and 2,2,2-trifluoro-1,1-bis(trifluoromethyl)-ethanol. We focused on determining rate constants of both high accuracy and precision so as to clearly delineate their temperature dependences.

2-Propanol (isopropyl alcohol, IPA) is an industrial chemical having relatively low toxicity (world production $\sim 2 \times 10^9$ kg/year⁵), which is widely used as a solvent (including consumer solvents), fuel additive (to remove water from gasoline), and chemical intermediate. The reaction between OH and $(\text{CH}_3)_2\text{CHOH}$ has been extensively studied since the mid 1970s.^{6–15} The room temperature data are consistent and the uncertainty of 10% and 20% at $T = 298$ K is currently recommended by the NASA/JPL¹⁶ and IUPAC Data Panels,¹⁷ respectively (95% confidence level). This uncertainty can probably be decreased based on the recent comprehensive study by Rajakumar et al.¹⁵ However, there are only two comprehensive studies of this reaction at temperatures of atmospheric interest (below room temperature),^{13,15} both indicating a weak negative temperature dependence of the rate constant, k_0 . The results of only one study of the reaction between OH and $(\text{CF}_3)_2\text{CHOH}$ are available.¹⁸ We are not aware of any study of reactions 3 and 4.

2. EXPERIMENTAL SECTION¹⁹

2.1. OH Reaction Rate Constant Measurements.

General descriptions of the apparatus and the experimental method used to measure the OH reaction rate constants are given in previous papers.^{20–23} Modifications to the apparatus and the measurement procedure, which resulted in significant improvements in the accuracy of the obtained kinetic data, were recently described in detail.^{23,24} In particular, the gas handling

system was completely rebuilt and a new reaction cell and photomultiplier installed.

The principal component of the flash photolysis-resonance fluorescence apparatus is a double-walled Pyrex reactor (of approximately 180 cm³ internal volume) equipped with quartz windows. The reactor is temperature controlled with methanol or water circulated between the outer walls. This reactor is located in a metal housing evacuated to prevent ambient water condensation during low temperature measurements. It also prevents extraneous absorption of the UV radiation from the flash lamp used to produce OH radicals. Reactions were studied in argon carrier gas at a total pressure of 4 kPa (30.0 Torr). Flows of dry argon, argon bubbled through water thermostatted at 276 K, and mixtures of each reactant (containing 0.02% to 1% of 2-propanol and 100% of other fluorinated alcohols) flowed through the reactor at a total flow rate between 0.21 and 2.4 cm³ s⁻¹, STP. The mixtures of 2-propanol diluted with Ar were prepared in a 10 L glass bulb equipped with Teflon/glass valve. Fluorinated alcohols were used as pure nondiluted compounds from smaller glass flasks equipped with Teflon valves. These storage flasks were thermostatted at temperatures between 3 and 14 °C during the experiment to maintain a stable vapor pressure of a compound in front of a flow controller and to prevent possible condensation of the compound in the gas handling system. The concentrations of the gases in the reactor were determined by measuring the gas flow rates and the total pressure with MKS Baratron manometers. Flow rates of argon, H₂O/argon mixture, and the reactant/argon mixture were measured and maintained using MKS mass flow controllers directly calibrated for every mixture. The calibration procedures for the mass flow controllers and manometers as well as the uncertainties associated with gas handling have been described in detail.²³ The total uncertainty of the kinetic results was estimated to be $\sim 2\%$ to 2.5% in the absence of chemical complications. The use of “High Accuracy Measurements” in the titles of our recent and present papers serves to emphasize the small instrumental uncertainty associated with measurements performed after the recent modification of the apparatus and in the measurement procedures.

Hydroxyl radicals were produced by the pulsed photolysis (2.5 to 10 Hz repetition rate) of H₂O, injected via the 276 K argon/water bubbler. The OH radicals were monitored by their resonance fluorescence near 308 nm, excited by a microwave-discharge resonance lamp (0.8 kPa or 6 Torr of a $\sim 2\%$ mixture of H₂O in UHP helium) focused into the reactor center. Resonantly scattered radiation from the center of the reaction cell was collimated by the reactor window/lens assembly and detected by a cooled photomultiplier (Type 9235, ET Enterprises, Ltd.) operating in the photon counting mode. The resonance fluorescence signal was recorded on a computer-based multichannel scaler (using a channel width of 100 μs) as a summation of 1000 to 20 000 consecutive flashes. The entire temporal OH profile was recorded and coadded following each flash, thereby minimizing any possible effects of small flash-to-flash variations on the initial OH concentration and drift in the detection radiation intensity.

In the absence of any reactant in the reactor, the temporal decay of OH concentration is associated with the net diffusion of OH out of the irradiation (photolysis) zone. This relatively long “background” decay was always recorded with a 2.5 Hz flash repetition rate to ensure in complete disappearance of the OH signal between consecutive flashes. These [OH] decays

were then recorded at various reactant concentrations with a flash repetition rate between 2.5 and 10 Hz. The procedure for deriving the reaction rate constant from such data has been described by Orkin et al.²¹ and in subsequent papers.^{23,25}

At each temperature the rate constant was determined from a fit to all of the decay rates obtained at that temperature. The temperatures for the measurements were chosen to be approximately equally distant along the Arrhenius $1/T$ scale in order to have them equally weighted in the fitting procedure. Experiments were always performed at two temperatures that are widely used in other studies, $T = 298$ and 272 K. The first one is standard room temperature, used in the evaluations and presentations of the rate constants while the second one is the temperature used in estimations of the atmospheric lifetime.²⁶ We increased the number of temperature points for the reaction between OH and $(\text{CH}_3)_2\text{CHOH}$ to better clarify the weak temperature dependence of the rate constant, k_0 .

In order to check for any complications, test experiments were performed at $T = 298$ K with the following variations of experimental parameters: the H_2O concentration (a factor of 4), the flash energy (a factor of 4), the flash repetition rate (a factor of 4), the residence time of the mixture in the reactor (a factor of 4), the reactant concentration in the storage bulb (a factor of 25 for iso-propanol, other compounds were not diluted), the residence time of this reactant mixture in the delivery volume between a storage bulb and a reactor (a factor of 4), and the total pressure in the reactor (a factor of more than 3, between 4 and 13.3 kPa (30–100 Torr)). No statistically significant changes in the measured reaction rate constant were observed in these test experiments. This is consistent with the results of our more intensive test experiments performed for the similar reaction between OH and ethanol.²⁴ Note that variations of the flash energy, the flash repetition rate, and H_2O concentration result in variations of reactant photolysis product accumulation, the OH concentration in the mixture and, therefore, reaction products accumulation. Through these test experiments we explored the possible influence of radical or stable products on the measured rate constant thereby enabling the appropriate choice of measurement conditions. The measurements performed with various gas flow rates and $(\text{CH}_3)_2\text{CHOH}$ concentrations in the storage bulb allowed checking for the potential absorption or desorption of the reactant in the gas handling system. Finally, the experiments at various pressures were done to check for a possible pressure dependence of the reaction rate constant.

2.2. Absorption Cross Sections Measurements. The IR absorption spectra were measured using a Nicolet 6700 FTIR spectrophotometer with spectral resolutions of 0.125 cm^{-1} (recorded with a step of 0.06 cm^{-1}) and 0.5 cm^{-1} (recorded with a step of 0.25 cm^{-1}). Both a liquid-nitrogen-cooled mercury–cadmium–tellurium detector (MCT) and a room temperature deuterated-triglycine-sulfate detector (DTGS) were used. The absorption cross sections obtained with these detectors were compared to avoid a possible systematic error due to differences in their properties. The DTGS detector, in particular, was used to obtain the reliable data in the longer wavelength region below 700 cm^{-1} where MCT detector could potentially introduce a systematic overestimation of the measured absorption cross sections.²³ A $10.2 \pm 0.05\text{ cm}$ glass absorption cell fitted with KBr windows was fixed in the spectrophotometer to minimize a baseline shift due to changes in the absorption cell position. The temperature of the cell was measured to be $295 \pm 1\text{ K}$. Between measurements the cell was

pumped out to $\sim 0.01\text{ Pa}$ and then filled with the gas to be studied. Absorption spectra of the evacuated cell and of the cell filled with a gas sample were alternately recorded several times, and the absorption cross sections at each wavenumber ν (cm^{-1}) were calculated. The experimental procedure and data treatment are similar to those described for UV absorption measurements. Details and potential complications of these measurements are discussed in a recent paper.²³ The overall instrumental error associated with the optical path length, pressure measurements, and temperature stability was estimated to be $\sim 0.5\%$. The uncertainty of the absorption measurements was usually less than $\sim 1\%$ except in the wavenumber region below $\sim 700\text{ cm}^{-1}$ where the spectrophotometer noise increases. All the measurements were done in pure fluorinated compounds sampled from the liquid phase with no bath gas added.

The UV absorption spectra of pure undiluted alcohols were obtained over the wavelength range of 164 to 200 nm using a single-beam apparatus consisting of a 1-m vacuum monochromator equipped with a 600 lines per mm grating. Spectra were recorded at increments of 0.5 nm at a spectral slit width of 0.16 nm. The pressure inside the two absorption cells used, 5.02 ± 0.01 or $46.71 \pm 0.05\text{ cm}$, was measured by a MKS Baratron manometer at $T = 295 \pm 1\text{ K}$. Absorption spectra of the evacuated cell and of the cell filled with a gas sample were alternately recorded several times, and the absorption cross sections at the wavelength λ were calculated as

$$\sigma(\lambda) = \frac{\ln\{I_0(\lambda)/I_{\text{ROH}}(\lambda)\}}{[\text{ROH}]L} \quad (5)$$

where $[\text{ROH}]$ is the concentration of the alcohol in the absorption cell with the optical path length L . I_0 and I_{ROH} are the radiation intensities measured after the absorption cell when the alcohol concentration was zero and $[\text{ROH}]$, respectively. The details can be found in an earlier publication.²⁴

Materials. The highest purity sample of 2-propanol was used as obtained from Fisher Scientific (stated purity of 99.9% with 10 ppm of acetone and less than 2 ppm of propionaldehyde being the main volatile reactive impurities and less than 0.02% of water). Samples of 1,1,1,3,3,3-hexafluoro-2-propanol were obtained from SynQuest Laboratories and Central Glass Co., Ltd. with stated purities of better than 99.9% with no reactive impurity detected. An additional sample with a stated purity of 99.7% was used in the test experiments and yielded no measurable difference. Four different samples of hexafluoro-2-methylisopropanol were obtained from SynQuest Laboratories with stated purities between 98.9% and 99.6%. In the purest sample 1,1,1,3,3,3-hexafluoro-2-propanol was the principal detected impurity. Four different samples of perfluoro-tert-butanol were obtained from SynQuest Laboratories with stated purities between 99.5% and 99.9% (hexafluoro-2-propanol and perfluoro propanone being identified as the main impurities). One sample of perfluoro-tert-butanol went through additional purification (distillation) for this study and six different fractions were obtained. The assay of the compound was 99.7% to 99.9% with amounts of more volatile and less volatile impurities varying by a factor of 2 to 3 among these fractions. The data presented in this paper were obtained with the sample of $(\text{CF}_3)_3\text{COH}$ in which the detected impurities have been best identified as hexafluoroacetone (0.06%), 1,1,1,4,4,4-hexafluoroobutanone (0.04%), 2-difluoromethyl-1,1,1,3,3,4,4,4-octafluoro-

2-methoxy-butane (0.02%), 1,1,1,3,3,3-hexafluoro-2-propanol (0.04%), and 0.04% of nonidentified deeply fluorinated (probably perfluorinated) saturated compound. All samples were carefully degassed via repeated freeze–pump–thaw cycles. We used 99.9995% and 99.9999% purity argon (Spectra Gases, Inc.) as a carrier gas.

3. RESULTS AND DISCUSSION

3.1. OH Reaction Rate Constants. The rate constants determined for the title reactions are presented in Tables 1 and

Table 1. Rate Constants Measured in the Present Work for the Reaction of OH with $(\text{CH}_3)_2\text{CHOH}^a$

<i>T</i> , K	$k_0(T) \times 10^{12}$, $\text{cm}^3 \text{ molecule}^{-1} \text{ s}^{-1}$	$[(\text{CH}_3)_2\text{CHOH}]$, $10^{13} \text{ molecule/cm}^3$	test experiments conditions
220	7.27 ± 0.05 (30)	0.38–3.8	
230	6.84 ± 0.08 (11)	0.62–3.7	
240	6.44 ± 0.10 (18)	0.54–3.2	
250	6.21 ± 0.06 (10)	0.63–4.3	
260	5.90 ± 0.07 (11)	0.61–4.2	
272	5.65 ± 0.04 (24)	0.55–4.2	
286	5.36 ± 0.06 (11)	0.60–4.2	
294	5.30 ± 0.04 (9)	0.60–4.8	
298	5.28 ± 0.03 (78)	0.59–5.0	
	5.30 ± 0.08		0.04 % mixture in the bulb
	5.32 ± 0.07		1 % mixture in the bulb
	5.32 ± 0.06		flow rate \approx 35%; [OH] \approx 200%
	5.36 ± 0.06		flow rate \approx 35%; [OH] \approx 600%
	5.25 ± 0.04		flash repetition rate = 50%
313	5.12 ± 0.06 (13)	0.61–4.2	
330	5.03 ± 0.07 (8)	0.62–4.8	
350	4.96 ± 0.07 (10)	0.61–4.6	
370	4.87 ± 0.04 (14)	0.61–4.8	
RRSD ^b	0.58%		

^aThe uncertainties are two standard errors from the least-squares fit of a straight line to the measured OH decay rates versus the reactant concentrations. They do not include the estimated instrumental/systematic uncertainty of ca. 1.5% to 2%. The bold data are results of the fit to all measurements performed at the particular temperature and 4.00 kPa (30.0 Torr) total pressure using a 0.2% mixture. These data are shown in Figure 1 and were used to derive the temperature dependences. The number of experiments is shown in parentheses for each temperature. ^bRelative residual standard deviation (RRSD)²⁴ is shown to uniformly represent the data deviation from the best fit temperature dependence.

2. The bold-highlighted data result from fits to all measurements performed at the indicated temperature under our “standard” experimental conditions: 4.00 kPa (30.0 Torr) total pressure, $\sim 6 \times 10^{14}$ molecule/cm³ of H₂O in the reactor, and ~ 0.1 J flash energy. These “standard” conditions, under which the kinetic results were not influenced by secondary reactions or other experimental complications, were selected based on the results from “test” experiments conducted in the present and previous work. The bold highlighted results are shown in the corresponding Figures 1 and 2 along with other available data for these reactions. The precision of our measurements allows clear resolution of curvature in the Arrhenius plots for all four reactions. The nature of this curvature is a subject of the

discussion and probably requires further (mechanistic) studies for complete resolution.

The results of some test experiments with iso-propanol mentioned earlier are also shown in Table 1 as the italicized text. These test experiment results indicate the absence of any effect of gas flow rate (the residence time of the mixture in the system) or of $(\text{CH}_3)_2\text{CHOH}$ concentration in the storage bulb on the measured rate constants. A barely measurable increase in the rate constant was observed only at a very high initial hydroxyl concentration (~ 6 times larger than that used under “standard” conditions). The test experiments performed at 13.3 kPa (100 Torr) revealed no change (less than 1%) in the measured reaction rate constant.

OH + (CH₃)₂CHOH. The results of our kinetic measurements for 2-propanol are presented in Table 1 and shown in Figure 1. The reaction rate constant has weak negative temperature dependence. We doubled the number of temperature points at which the rate constant was measured to allow better visualization of the data scattering and clear resolution of the curvature in the Arrhenius plot. A three-parameter modified Arrhenius dependence fit to the bold highlighted data set in Table 1 is shown by the curved dotted line in Figure 1

$$k_0(220 - 370 \text{ K}) = 3.84 \times 10^{-13} (T/298)^{1.99} \exp\{+781/T\} \quad (6)$$

The temperature dependence of $k_0(T)$ can be presented equally well as the sum of two Arrhenius expressions shown in Figure 1 with the solid and dashed lines

$$k_0(220 - 370 \text{ K}) = 1.456 \times 10^{-11} \exp\{-883/T\} + 1.30 \times 10^{-12} \exp\{+371/T\} \quad (7)$$

In both cases the statistical uncertainties of individual data points presented in Table 1 were used for weighted fits. Note that the data scattering around the fitted line is consistent with the reported uncertainties of individual data points as illustrated in the lower panel of Figure 1. The data quality allows one to apply a statistical ChiSquare test, which yields a very significant deviation from the straight two-parameter Arrhenius dependence. Both expressions 6 and 7 are quite adequate to represent the data set. The characteristic data deviation from the fitted line can be numerically represented by the relative residual standard deviation (RRSD)²⁴

$$\text{RRSD} = \sqrt{\frac{\sum_{j=1}^N (\Delta k_j/k(T_j))^2}{(N-p)}} = 0.58\% \quad (8)$$

where Δk_j is a deviation of the measured rate constant from the best fit curve, $k(T_j)$, N is the number of measured rate constants used in the fit, and p is the number of fitted parameters in the suggested expression.

The room temperature rate constant determined in this study can be presented as

$$k_0(298 \text{ K}) = (5.28 \pm 0.13) \times 10^{-12} \text{ cm}^3 \text{ molecule}^{-1} \text{ s}^{-1} \quad (9)$$

The indicated total uncertainty represents a 95% confidence level, which includes the statistical two standard errors combined with the estimated instrumental uncertainty. The presence of identified impurities (acetone (10 ppm) and propionaldehyde (2 ppm)) can result in an error of less than 0.001% based on their reactivity toward OH.¹⁶

Table 2. Rate Constants Measured in the Present Work for the Reaction of OH with $(\text{CF}_3)_2\text{CHOH}$, $(\text{CF}_3)_2\text{C}(\text{OH})\text{CH}_3$, and $(\text{CF}_3)_3\text{COH}^a$

T, K	$k_1(T) \times 10^{14}, \text{cm}^3 \text{molecule}^{-1} \text{s}^{-1}$	$[(\text{CF}_3)_2\text{CHOH}], 10^{16} \text{molecule}/\text{cm}^3$	$k_2(T) \times 10^{15}, \text{cm}^3 \text{molecule}^{-1} \text{s}^{-1}$	$[(\text{CF}_3)_2\text{C}(\text{OH})\text{CH}_3], 10^{16} \text{molecule}/\text{cm}^3$	$k_3(T) \times 10^{16}, \text{cm}^3 \text{molecule}^{-1} \text{s}^{-1}$	$[(\text{CF}_3)_3\text{COH}], 10^{16} \text{molecule}/\text{cm}^3$
220	1.27 ± 0.03 (17)	0.08–0.32				
230	1.32 ± 0.02 (55)	0.21–0.93	4.63 ± 0.07 (12)	0.25–1.1	9.8 ± 0.3 (8)	0.34–2.3
240	1.41 ± 0.02 (22)	0.22–1.22				
250	1.53 ± 0.02 (26)	0.16–1.38	5.03 ± 0.17 (13)	0.42–2.0	8.5 ± 0.4 (8)	0.59–2.3
272	1.92 ± 0.02 (15)	0.15–1.25	5.85 ± 0.11 (12)	0.35–1.7	8.0 ± 0.2 (14)	0.60–2.8
298	2.47 ± 0.03 (39)	0.15–0.92	7.84 ± 0.12 (29)	0.25–1.2	8.6 ± 0.2 (18)	0.28–2.3
330	3.42 ± 0.02 (27)	0.09–0.77	11.2 ± 0.5 (10)	0.25–0.99	10.3 ± 0.1 (9)	0.57–2.0
370	4.86 ± 0.04 (42)	0.28–1.04	18.2 ± 0.3 (11)	0.12–0.75	13.1 ± 0.5 (17)	0.57–2.3
RRSD ^b	0.84%		1.4%		2.5%	

^aThe uncertainties are two standard errors from the least-squares fit of a straight line to the measured OH decay rates versus the reactant concentrations and do not include the estimated systematic uncertainty. The number of experiments is shown in parentheses for each temperature.

^bRelative residual standard deviation (RRSD) given by the expression 8 is shown to uniformly represent the data deviation from the best fit temperature dependence.

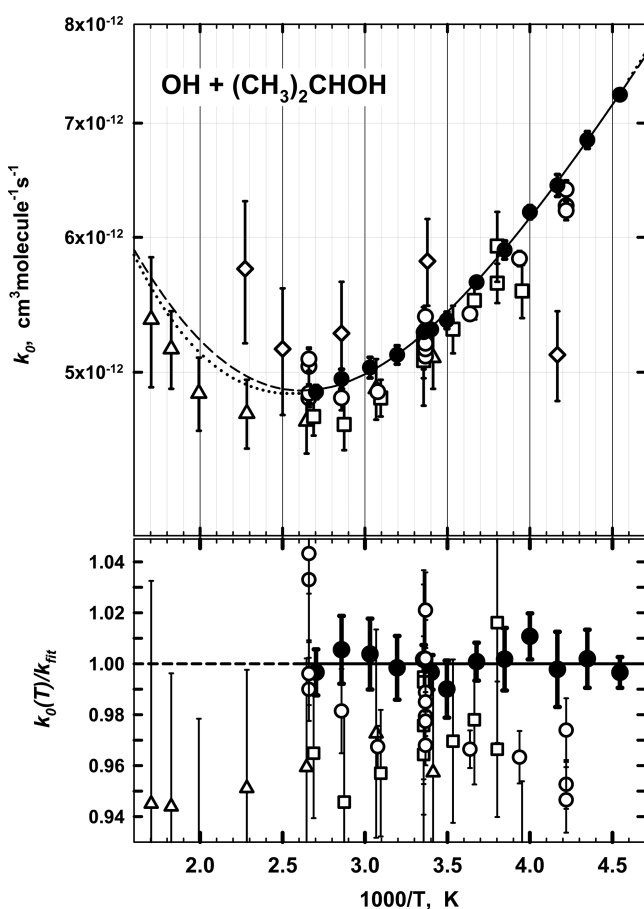


Figure 1. Available results of the rate constant measurements extended beyond room temperature for the reaction between OH and 2-propanol, $k_p(T)$: (\diamond) Wallington and Kurylo,¹⁰ (Δ) Dunlop and Tully,¹² (\square) Yujing and Mellouki,¹³ (\circ) Rajakumar et al.,¹⁵ and (\bullet) this study. The lower panel shows the same data normalized by the best fit to the data from this study, expression 7.

The data available for this reaction are summarized in Table 3. The room temperature data obtained in all studies are in very good agreement and coincide with our value within the reported uncertainties. This reaction is fast enough and 2-propanol is a common industrial chemical with a long history of manufacturing. Therefore, we can assume that the samples of 2-propanol used in prior studies were also pure enough so that

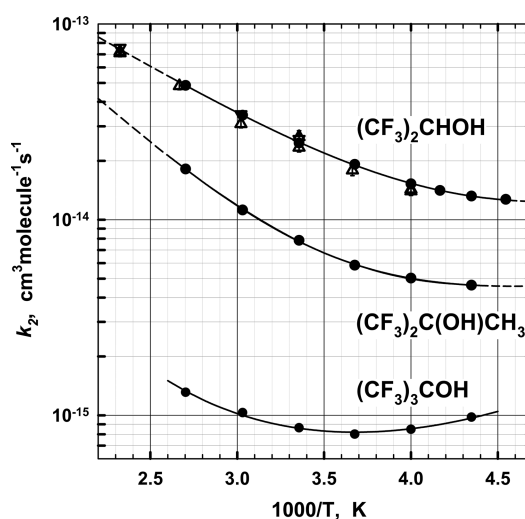


Figure 2. Results of rate constant measurements for the reactions between OH and $(\text{CF}_3)_2\text{CHOH}$, $(\text{CF}_3)_2\text{C}(\text{OH})\text{CH}_3$, and $(\text{CF}_3)_3\text{COH}$: (Δ, ∇) pulsed photolysis experiments and discharge flow experiments respectively from Tokuhashi et al.¹⁸ and (\bullet) this study.

the reactive impurities were not a problem in these previous measurements. Therefore, differences in the measured reaction rate constants most likely reflect differences among kinetic apparatuses and associated procedures. The reported central values from all recent absolute rate constant measurements at room temperature span a range of only $\sim 4\%$.

While the data of the very first study¹⁰ of the temperature dependence are somewhat scattered, the results of two later studies^{13,15} that extended measurements below room temperature are in rather good agreement. These data lie only a few percent below our results with the scattering and statistical uncertainty of individual points being of the same values. This is illustrated in the lower panel of Figure 1 where the data points are presented after normalization by expression 7 along with their relative uncertainties. Both Yujing and Mellouki¹³ and Rajakumar et al.¹⁵ used a standard two-parameter Arrhenius expression to represent the measured reaction rate constant. Table 3 also shows the results of our three-parameter Arrhenius fit to the data set from Rajakumar et al.,¹⁵ which represents the data better than a standard Arrhenius expression and is very similar to the three-parameter Arrhenius fit to our

Table 3. Reported Results on the Rate Constants of the OH Reactions with $(\text{CH}_3)_2\text{CHOH}$ and $(\text{CF}_3)_2\text{CHOH}^a$

molecule	$k(298 \text{ K}) \times 10^{12}$ $\text{cm}^3 \text{ molecule}^{-1} \text{ s}^{-1}$	temperature dependence	temperature range, K	technique	ref
$(\text{CH}_3)_2\text{CHOH}$	4.7		305	RR-GC	6 ^b
	6.9 ± 2.1		305 (± 2)	RR	7 ^c
	5.48 ± 0.55		296 (± 2)	FP-RA	8
	4.6		300	RR-GC	9
	5.35 ± 0.35	$5.8 \times 10^{-12} \exp\{-23 \pm 87/T\}$	240–440	FP-RF	10
	5.69 ± 1.09		298 (± 2)	PR-RA	11
	5.38 ± 0.70		298 (± 2)	RR-GC	11
	5.07 ± 0.23	$4.3 \times 10^{-13} (T/298)^{1.87} \exp(739/T)$	293–587	PLP-LIF	12
	5.18 ± 0.077	$2.8 \times 10^{-13} \exp\{(183 \pm 40)/T\}$	253–372	PLP-LIF	13
	5.23 ± 0.39		295 (± 2)	RR-GC	14
	5.32 ± 0.087	$2.9 \times 10^{-13} \exp\{(174 \pm 34)/T\}$	237–376	PLP-LIF	15
	5.16 ± 0.20	$3.52 \times 10^{13} (T/298)^{2.16} \exp(800/T)$			15, our fit
	5.28 ± 0.13	$1.46 \times 10^{11} \exp(-883) + 1.30 \times 10^{13} \exp(781/T)$	220–370	FP-RF	this work
		$3.84 \times 10^{13} (T/298)^{1.99} \exp(781/T)$	220–370		
	$(\text{CF}_3)_2\text{CHOH}$	$(2.53 \pm 0.11) \times 10^{-2}$	$7.0 \times 10^{-13} \exp\{-988 \pm 62/T\}$	250–430	PLP/DF-LIF
$(2.49 \pm 0.09) \times 10^{-2}$		$5.0 \times 10^{-13} \exp\{-893 \pm 78/T\}$	250–375		18
$(2.49 \pm 0.06) \times 10^{-2}$		$1.19 \times 10^{12} \exp(-1207) + 7.85 \times 10^{16} \exp(502/T)$	220–370	FP-RF	this work
		$9.05 \times 10^{17} (T/298)^{8.86} \exp(1674/T)$	220–298		
$(2.60 \pm 0.11) \times 10^{-2}$		$5.4 \times 10^{-13} \exp\{-904 \pm 86/T\}$	250–370		

^aUncertainties are either from the original papers or represent two standard error from our fit to the original data. The uncertainties of $k(298 \text{ K})$ shown with bold highlighted text are the total uncertainties for the rate constants obtained in this work, which include two standard error and the estimated instrumental uncertainty. $k(298 \text{ K})$ are calculated from the fit to the entire data set of a particular study. The rate constants measured at the single temperature (refs 6–9 and 14) are presented at the temperature of the original study with no correction to $T = 298 \text{ K}$. ^bRecalculated using the current recommendation for the rate constant of the reference reaction with toluene.¹⁷ ^cRecalculated using the current recommendation for the rate constant of the reference reaction with isobutene.¹⁷

data. The data reported by Dunlop and Tully¹² at room temperature and above also suggested curvature in the Arrhenius plot. Both expressions 6 and 7 obtained from the fit to our data describe quite well the trend of the rate constant when extrapolated to the higher temperatures beyond our measurements range (shown with the dashed (7) and dotted (6) lines in Figure 1). The data of Dunlop and Tully¹² obtained between 293 and 587 K are only ~5% systematically below the prediction by either expression. We observed a similar comparison result in our study of the reaction between OH and $\text{CH}_3\text{CH}_2\text{OH}$.^{24,27} A three-parameter fit to the data of Dunlop and Tully¹² returns parameters that are very similar to those in eq 6, see Table 3. Although the success of these extrapolations may be considered as coincidental, it does lend credibility to the moderate extrapolation of a smooth dependence when the goodness of the fit is sufficiently high.

OH + $(\text{CF}_3)_2\text{CHOH}$. The results of our measurements are presented in Table 2 and shown in Figure 2. The Arrhenius plot exhibits a curvature that is clearly resolved in our experiments. In contrast with the case of $k_0(T)$ discussed above, a three-parameter modified Arrhenius expression does not do as good a job at fitting the data for this reaction as does a sum of two Arrhenius expressions.

$$k_1(220 - 370 \text{ K}) = 1.19 \times 10^{-12} \exp\{-1207/T\} + 7.85 \times 10^{-16} \exp\{+502/T\} \quad (10)$$

This expression yields RRSD = 0.84%, which is consistent with the uncertainties of individual data points. The best three-parameter expression, $k_2(T) = A(T/298)^n \exp\{-E/RT\}$, results in a larger RRSD = 3.2% substantially exceeding individual uncertainties reported in Table 2. However, the three-parameter fit can be used to represent $k_1(T)$ at temperatures

of atmospheric interest, i.e., below room temperature (RRSD = 0.59%)

$$k_1(220 - 298 \text{ K}) = 9.05 \times 10^{-17} (T/298)^{8.86} \exp\{+1674/T\} \quad (11)$$

The room temperature rate constant determined in this study can be presented as

$$k_1(298 \text{ K}) = (2.49 \pm 0.06) \times 10^{-14} \text{ cm}^3 \text{ molecule}^{-1} \text{ s}^{-1} \quad (12)$$

The indicated total uncertainty represents a 95% confidence level, which include the statistical two standard errors combined with the estimated instrumental uncertainty.

The only other study of this reaction was performed by an absolute technique between 250 and 430 K using both pulsed laser photolysis and discharge flow to generate OH and LIF to follow the kinetics of its decay.¹⁸ The results of this study are also shown in Figure 2 using different symbols to distinguish between the pulsed and flow approaches. Our results are in excellent agreement with those reported by Takuhashi et al.¹⁸ over the common temperature range. Table 3 show $k_1(298)$ and Arrhenius temperature dependences obtained from the fit to our data and those from ref 18 between 250 and 375 K. However, our data exhibit a statistically significant curvature even over this restricted range of temperatures. The attempt to fit the Arrhenius expression to the data yields RRSD = 4.9%, which is much larger than the uncertainties of individual points in Table 2.

The temperature dependence of $k_1(T)$ exhibits a noticeable leveling off at lower temperatures. We measured the rate constant at an additional temperature point, $T = 240 \text{ K}$, to check this trend. This behavior is likely indicative of a change in reaction mechanism and possibly of the reaction site being

attacked by OH. It can also be due to the formation of a short-lived intermediate reaction complex or to tunneling.

$\text{OH} + (\text{CF}_3)_2\text{C}(\text{OH})\text{CH}_3$. The results of our measurements are presented in Table 2 and shown in Figure 2. A fit of the sum of two Arrhenius expressions to our data results in the following expression (RRSD = 1.4%)

$$k_2(230 - 370 \text{ K}) = 1.675 \times 10^{-12} \exp\{-1718/T\} + 7.32 \times 10^{-16} \exp\{+371/T\} \quad (13)$$

The room temperature rate constant determined in this study can be presented as

$$k_2(298 \text{ K}) = (7.84 \pm 0.23) \times 10^{-15} \text{ cm}^3 \text{ molecule}^{-1} \text{ s}^{-1} \quad (14)$$

where the indicated total uncertainty represents a 95% confidence level, which include the statistical two standard errors combined with the estimated instrumental uncertainty. The presence of reactive impurities is a potential source of overestimating the reaction rate constant measured by an absolute technique. The main detected impurity (1,1,1,3,3,3-hexafluoro-2-propanol) is ~ 2.8 times more reactive toward OH than the compound under study, see Table 2. The presence of this impurity in the detected amount of 0.4% should result in less than 1% overestimation of the measured reaction rate constant, $k_2(T)$. We studied three different samples of this compound with different levels of detected impurities. No substantial variation of the rate constant measured at 298 and 230 K was observed. We conservatively estimate the uncertainty of this measured rate constant to be $\sim 5\%$ at room temperature and less than 10% at the lowest temperatures. Nevertheless, complementary measurements using a relative rate technique would be very supportive. We are unaware of any other studies of this reaction.

$\text{OH} + (\text{CF}_3)_3\text{COH}$. The results of our measurements are presented in Table 2 and shown in Figures 2 along with those for $(\text{CF}_3)_2\text{CHOH}$ and $(\text{CF}_3)_2\text{C}(\text{OH})\text{CH}_3$. The reaction is very slow and the range of the rate constant variation is surprisingly small. We use a three-parameter Arrhenius dependence to present this rate constant

$$k_3(230 - 370 \text{ K}) = 3.0 \times 10^{-20} (T/298)^{11.3} \exp\{+3060/T\} \quad (15)$$

The expression is a result of a weighted fit assuming the same relative precision for all data points. The room temperature rate constant determined in this study can be presented as

$$k_3(298 \text{ K}) = (8.6 \pm 0.8) \times 10^{-15} \text{ cm}^3 \text{ molecule}^{-1} \text{ s}^{-1} \quad (16)$$

where the indicated total uncertainty represents a 95% confidence level, which include the statistical two standard errors, the estimated instrumental uncertainty, and the variation in of the results obtained with different samples. Based on their reactivity toward OH, the identified impurities in the sample of $(\text{CF}_3)_3\text{COH}$ used to obtain $k_3(T)$ do not affect the data reported in Table 2. Although the reactivity of hexafluoroacetone toward OH is not available, $(\text{CF}_3)_2\text{CO}$ should not undergo reaction since there is no obvious reaction channel. The reactivity of CF_3COCH_3 ²⁸ can be used instead to obtain 0.3% as a very conservative estimate of an upper limit for an error due to the presence of 0.06% of $(\text{CF}_3)_2\text{CO}$. 1,1,1,3,3,3-hexafluoro-2-propanol $(\text{CF}_3)_2\text{CHOH}$, in the amount of 0.04%

contributes $\sim 1.5\%$ to the measured rate constant at $T = 370 \text{ K}$ and $\sim 0.5\%$ at $T = 230 \text{ K}$, based on results of this study. The reactivity of 2-difluoromethyl-1,1,1,3,3,4,4,4-octafluoro-2-methoxy-butane, which can be presented as $\text{CH}_3\text{-O-C}(\text{CF}_3)\text{-}(\text{C}_2\text{F}_5)\text{-CHF}_2$, toward OH can be assumed to be similar to that of the similar fluorinated ether, $\text{CH}_3\text{-O-CF}_2\text{-CHF}_2$.¹⁶ Therefore, a 0.02% impurity of this compound contributes $\sim 0.8\%$ to the measured rate constant at $T = 370 \text{ K}$ and much less at lower temperatures. There are no data on the reaction between OH and $\text{CF}_3\text{CH}_2\text{C}(\text{O})\text{CF}_3$ (1,1,1,4,4,4-hexafluorobutanone). The rate constant of the reaction between OH and non-substituted 2-butanone, $\text{CH}_3\text{CH}_2\text{C}(\text{O})\text{CH}_3$, has a very weak temperature dependence and $k(298 \text{ K}) = 1.1 \times 10^{-12} \text{ cm}^3 \text{ molecule}^{-1} \text{ s}^{-1}$.¹⁷ We can estimate the deactivating effect of CF_3 substitution on the reactivity of an adjacent CH_2 group in 2-butanone based on reactivity change of other compounds due to similar fluorination:^{16,17} $\text{CF}_3\text{CH}_2\text{CH}_2\text{CF}_3/\text{n-C}_4\text{H}_{10}$ (a factor of 320), $\text{CF}_3\text{CH}_2\text{OCH}_2\text{CF}_3/\text{C}_2\text{H}_5\text{OC}_2\text{H}_5$ (a factor of 80), $\text{CF}_3\text{CH}_2\text{OH}/\text{C}_2\text{H}_5\text{OH}$ (a factor of 34). These data suggest that a 0.04% impurity of $\text{CF}_3\text{CH}_2\text{C}(\text{O})\text{CF}_3$ probably contributes less than 1% to the measured rate constant k_3 . The effect of the nonidentified impurity ($\sim 0.04\%$) cannot be quantified. However, a saturated perfluorinated compound would not react with OH and, therefore, cannot affect our results. Even the reactivity of any deeply fluorinated saturated compound toward OH is relatively slow¹⁶ and the effect of such an impurity on the results of our measurements can be assumed to be similar to the above estimated effects of identified impurities. We studied different samples of $(\text{CF}_3)_3\text{COH}$ with different levels of detected impurities. The results obtained with the purest samples were consistent when test experiments were performed at 298 and 370 K. However, the detection and identification of small amounts of fluorinated impurities often poses a problem, which can result in overestimation of the measured reaction rate constant. Therefore, complementary studies of this reaction using a relative rate technique would be very supportive. This is the first direct measurement of the rate constant of H-abstraction from the COH group of fluorinated alcohol and suggests an unusually weak temperature dependence for such slow reaction.

Discussion of Kinetics. The Arrhenius plots for all four reactions exhibit a noticeable curvature clearly resolved in our study. Note that a curvature of the Arrhenius plot is not that uncommon: it has been resolved in a number of cases where precise data are available over the sufficient temperature range.^{23,24,29-31} In particular, it was observed for the reactions between OH and smaller fluorinated alcohols – ethanols.²⁴

2-Propanol is slightly more reactive toward OH than ethanol (a factor of ~ 1.6 at room temperature) with a different temperature dependence. Its reaction rate constant visibly increases with lowering the temperature below ca. 400 K (see Figure 1), whereas the OH reaction rate constant of ethanol essentially levels off at temperatures of atmospheric interest (i.e., below room temperature).²⁴ Note that both reactions are relatively fast.

Fluorination of the α -carbon with CF_3 substantially decreases the reactivity of alcohols toward hydroxyl radicals. H-atom abstraction from the α -carbon, a methylene group, CH_2 , is the main channel for the OH reaction with ethanol.³² Similarly, H-abstraction from the CH group probably dictates the reactivity of both 2-propanol, $(\text{CH}_3)_2\text{CHOH}$, and hexafluoro-2-propanol, $(\text{CF}_3)_2\text{CHOH}$. Thus a two CF_3 substitution in 2-propanol decreases the reactivity of CH group by a factor of ~ 210 . This

is somewhat consistent with the pronounced deactivating effect of CF_3 substitution in ethanol, where a single CF_3 group decreases the reactivity of CH_2 group by a factor of 34. $(\text{CF}_3)_2\text{CHOH}$ can be considered as $\text{CF}_3\text{CH}_2\text{OH}$ substituted with CF_3 at the α -carbon. Such substitution with a second CF_3 results in a reactivity decrease of an additional factor of 4 (or a factor of 2 if one considers the reactivity per H-atom). The methyl group in $(\text{CF}_3)_2\text{C}(\text{OH})\text{CH}_3$ is less reactive than the CH group in $(\text{CF}_3)_2\text{CHOH}$ by a factor of ~ 3 . However, it is still at least an order of magnitude more reactive at room temperature than the OH group in $(\text{CF}_3)_3\text{COH}$.

The curvature of the Arrhenius plots for reactions 2 and 3 can be attributed to the complex mechanism of these elementary reactions including the effect of tunneling and the contribution from the H-atom abstraction from OH group of fluorinated alcohols. For example, Wang et al.³³ conducted ab initio modeling of the OH reaction with $\text{CF}_3\text{CH}_2\text{OH}$ to find a curvature in the Arrhenius plot due to different reactivities of the two reaction sites (CH_2 and OH) with tunneling playing an important role and resulting in the very weak temperature dependence of the second channel at lower temperatures.

$(\text{CF}_3)_3\text{COH}$ has been studied in the attempt to estimate the environmental properties of this long-lived compound and to estimate the rate constant of H-abstraction from the OH group by hydroxyl. Because the α -carbon in ethanol cannot be fluorinated, $(\text{CF}_3)_3\text{COH}$ is the simplest fully halogenated alcohol with OH being the only reactive group. The above-mentioned strong effect of tunneling may explain the temperature independent reaction rate constant $k_3(T)$ obtained in our study assuming that these results are not entirely due to the presence of nonrecognized, very reactive impurities in the samples of perfluoro-tert-butanol. If one accepts such a weak temperature dependence for H-abstraction from the OH group of fluorinated alcohol, this can be applied to explain the temperature dependence of rate constants for OH reactions of other fluorinated alcohols, $k_1(T)$ and $k_2(T)$. Additional studies of this reaction via complementary techniques would be helpful. The availability of experimental data should stimulate further theoretical studies to improve our understanding of chemical mechanisms and the development of predictive computational tools.

3.2. IR Absorption Spectra. The IR absorption spectra of three fluorinated alcohols are presented in Figures 3–5. The spectra were combined as described earlier from the results of measurements at various pressures of compounds restricted by their saturated vapor pressures: 0.4 to 6.4 kPa (3 to 48 Torr) for $(\text{CF}_3)_2\text{CHOH}$, 0.21 to 13.6 kPa (1.6 to 102 Torr) for $(\text{CF}_3)_2\text{C}(\text{OH})\text{CH}_3$, and 0.17 to 5.5 kPa (1.3 to 41 Torr) for $(\text{CF}_3)_3\text{COH}$. The top panels in these figures show the spectra obtained with a spectral resolution of 0.125 cm^{-1} to illustrate the main absorption features. The lower panels show the same spectra recorded with a spectral resolution of 0.5 cm^{-1} in log scale to illustrate smaller absorption features. IR absorption cross sections are available in the Supporting Information. The IR spectra of these fluorinated C3–C4 alcohols do not exhibit any narrow spectral absorption features and spectra obtained with different spectral resolutions are in good agreement. We are not aware of any reported IR data for these compounds.

3.3. UV Absorption Spectra. The ultraviolet absorption spectra obtained in this work are presented in Figure 6 with solid lines. The spectra of ethanol²⁴ and 2,2,2-trifluoroethanol $(\text{CF}_3\text{CH}_2\text{OH})$ ²⁴ are plotted with dashed lines for comparison. As we noted in case of fluorinated ethanols, fluorination causes

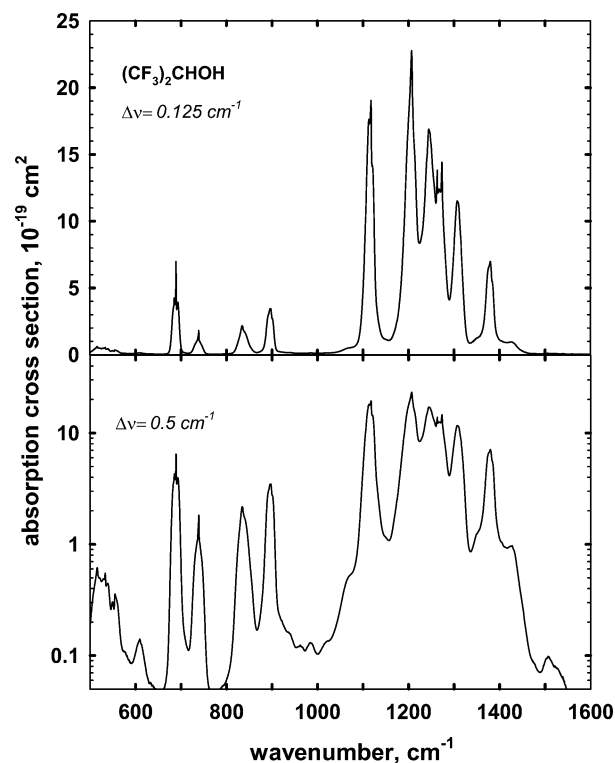


Figure 3. IR absorption spectrum of 1,1,1,3,3,3-hexafluoro-2-propanol, $(\text{CF}_3)_2\text{CHOH}$, obtained with a spectral resolution of 0.125 (top panel) and 0.5 cm^{-1} (lower panel). The latter is shown in log scale to better visualize smaller absorption features.

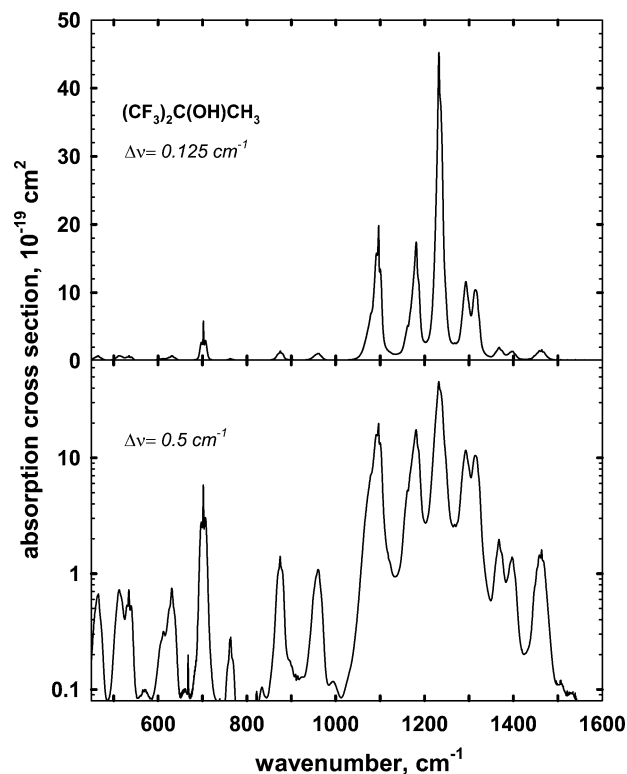


Figure 4. IR absorption spectrum of 1,1,1,3,3,3-hexafluoro-2-methyl-2-propanol, $(\text{CF}_3)_2\text{C}(\text{OH})\text{CH}_3$, obtained with a spectral resolution of 0.125 (top panel) and 0.5 cm^{-1} (lower panel). The latter is shown in log scale to better visualize smaller absorption features.

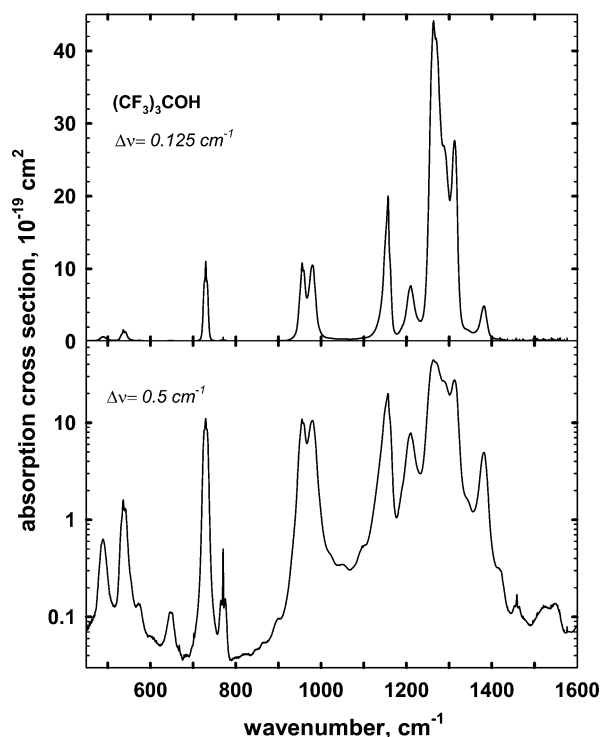


Figure 5. IR absorption spectrum of and 1,1,1,3,3,3-hexafluoro-2-(trifluoromethyl)-2-propanol (perfluoro-tert-butanol), $(\text{CF}_3)_3\text{COH}$, obtained with a spectral resolution of 0.125 (top panel) and 0.5 cm^{-1} (lower panel). The latter is shown in log scale to better visualize smaller absorption features.

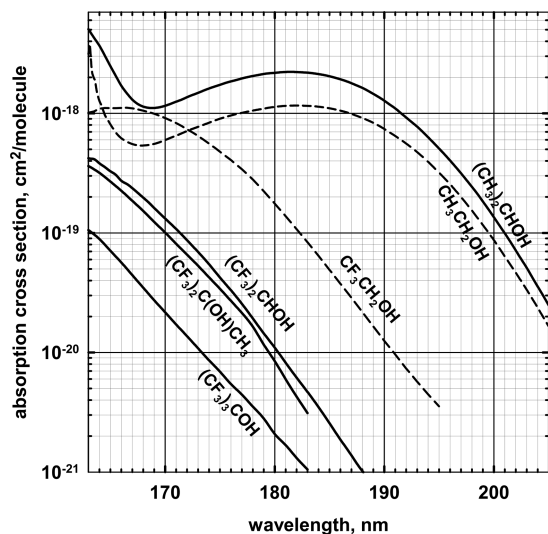


Figure 6. UV absorption spectra obtained in this study for iso-propanol and fluorinated alcohols. UV absorption spectra of ethanol and $\text{CF}_3\text{CH}_2\text{OH}$ are from Orkin et al.²⁴

a “blue shift” of the absorption band that results in a significant decrease in the absorption at the particular wavelength. Thus, the second CF_3 group added to $\text{CF}_3\text{CH}_2\text{OH}$ results in about an order of magnitude decrease in absorption and the third CF_3 group further decreases it by a factor of 5. At the same time, CH_3 substitution causes no substantial change of UV absorption. The absorption spectra of ethanol and iso-propanol are very similar as are those of $(\text{CF}_3)_2\text{CHOH}$ and $(\text{CF}_3)_2\text{C}(\text{OH})\text{CH}_3$.

Harrison et al.³⁴ reported extinction coefficients of $(\text{CH}_3)_2\text{CHOH}$ at its absorption minimum near 168 nm and absorption maximum near 181 nm, which are 11% smaller and 7% larger than our values, respectively. This is actually reasonably good agreement for experiments employing quantitative photometry of photo plates.³⁴ Salahub and Sandorfy³⁵ reported the extinction coefficient near the 182 nm maximum, which exceeds our value by only ~3%. The same good agreement extends down to 175 nm; however, the discrepancy is larger at both shorter and longer wavelengths.³⁵ Recently, Rajakumar et al.¹⁵ reported an absorption cross section of iso-propanol at the mercury line, 184.9 nm, which is smaller than our value by ~5% although within the combined uncertainty. Salahub and Sandorfy's³⁵ original graphic results digitized by Keller-Rudek and Moortgat³⁶ are the only available UV absorption data for $(\text{CF}_3)_2\text{CHOH}$ and exceed our results by 20% to 50% over 162 to 178 nm, respectively. Salahub and Sandorfy³⁵ reported the maximum absorption of $(\text{CF}_3)_2\text{CHOH}$ at 154.5 nm beyond the range of our measurements, $\sigma(154.5 \text{ nm}) = 9.44 \times 10^{-19} \text{ cm}^2/\text{molecule}$. This value is very similar to the absorption intensity of $\text{CF}_3\text{CH}_2\text{OH}$ at its maximum located at 165 nm^{35,24} thus supporting the observation that the main effect of fluorination on UV absorption is a “blue shift” of the absorption band with little effect on its maximum intensity. We are unaware of any UV absorption data for $(\text{CF}_3)_2\text{C}(\text{OH})\text{CH}_3$ and $(\text{CF}_3)_3\text{COH}$.

4. ATMOSPHERIC IMPLICATIONS

The atmospheric lifetimes of alcohols due to their reactions with tropospheric hydroxyl radicals, τ_i^{OH} , can be estimated using a simple scaling procedure that is based on the results of field measurements³⁷ and thorough atmospheric modeling²⁶

$$\tau_i^{\text{OH}} = \frac{k_{\text{MCF}}(272)}{k_i(272)} \tau_{\text{MCF}}^{\text{OH}} \quad (17)$$

where τ_i^{OH} and $\tau_{\text{MCF}}^{\text{OH}}$ are the lifetimes of a compound under study and methyl chloroform, respectively, due to reactions with hydroxyl radicals in the troposphere only, and $k_i(272 \text{ K})$ and $k_{\text{MCF}}(272 \text{ K}) = 6.14 \times 10^{-15} \text{ cm}^3 \text{ molecule}^{-1} \text{ s}^{-1}$ are the rate constants for the reactions of OH with these substances at $T = 272 \text{ K}$ given by the expressions 7, 10, 13, 15 and in ref 16, respectively. The value of $\tau_{\text{MCF}}^{\text{OH}} = 6.0$ years was obtained from the measured lifetime of MCF of 4.9 years when an ocean loss of 89 years and a stratospheric loss of 39 years were taken into account. Applying this method to the title compounds of this study yields estimated atmospheric lifetimes of 2.4 days and 1.9, 6.3, and 45.5 years for 2-propanol, 1,1,1,3,3,3-hexafluoro-2-propanol, 1,1,1,3,3,3-hexafluoro-2-methyl-2-propanol, and perfluoro-tert-butanol, respectively. These lifetimes can be further shortened if wet deposition plays a significant role in the atmospheric removal of these compounds. UV photolysis cannot affect the lifetime of these compounds. The estimated atmospheric lifetime of 2-propanol is significantly shorter than the characteristic time of mixing processes in the troposphere and hence is only crude estimate, which can be used for comparison with other very short-lived substances (VSLs).

In contrast with very short-lived 2-propanol, the fluorinated alcohols studied in this work have sufficiently long lifetimes comparable or exceeding the characteristic times of atmospheric mixing. We can make simplified estimations of the global warming potentials of fluorinated ethanols by combining their estimated atmospheric lifetimes, measured IR absorption

spectra, and the measured spectrum of Earth's outgoing radiation. This estimation procedure was described in our earlier papers^{38,39} and yielded results that compared favorably with other simplified estimations and with more rigorous atmospheric model calculations of GWPs.^{23,39} We calculate GWPs in two steps. First, we calculate a halocarbon global warming potential (HGWP) using CFC-11 (CFCl₃) as a relative compound with no other modeling data being used at this stage. Second, we use the GWP of CFC-11 relative to CO₂ obtained from rigorous radiative transfer modeling¹ to calculate the GWPs of our compounds relative to CO₂. Table 4 presents the results of these GWP estimations for time horizons of 20, 100, and 500 years, respectively.

Table 4. Atmospheric Lifetimes of Fluorinated Alcohols and Their Direct GWPs

molecule	atmospheric lifetime, years	GWPs at time horizons:		
		20 years	100 years	500 years
(CF ₃) ₂ CHOH	1.94	830	240	72
(CF ₃) ₂ C(OH)CH ₃	6.27	2410	710	220
(CF ₃) ₃ COH	45.5	6360	4520	1550

■ ASSOCIATED CONTENT

Ⓢ Supporting Information

UV absorption cross sections and IR absorption cross sections of fluorinated compounds. This material is available free of charge via the Internet at <http://pubs.acs.org>.

■ AUTHOR INFORMATION

Corresponding Author

*E-mail: vladimir.orkin@nist.gov.

Notes

The authors declare no competing financial interest.

■ ACKNOWLEDGMENTS

This work was supported by the Upper Atmosphere Research Program of the National Aeronautics and Space Administration and NIST Measurement Services Advisory Group. Authors thank Dr. Adam Alty, Christopher J. Deigl, and Douglas B. Tatham of SynQuest Laboratories, Inc. for their help with sample analyses and purity discussions. V.L.O. acknowledges the support of NATO CLG Program, Grants ES-P.EAP.CLG.983035 and EST.CLG979421.

■ REFERENCES

- (1) Global Ozone Research and Monitoring Project - Report No. 52 Scientific Assessment of Ozone Depletion; World Meteorological Organization, 2010, pp 516.
- (2) Velders, G. J. M.; Andersen, S. O.; Daniel, J. S.; Fahey, D. W.; McFarland, M. The importance of the Montreal Protocol in protecting climate. *Proc. Natl. Acad. Sci.* **2007**, *104* (12), 4814–4819.
- (3) Velders, G. J. M.; Fahey, D. W.; Daniel, J. S.; McFarland, M.; Andersen, S. O. The large contribution of projected HFC emissions to future climate forcing. *Proc. Nat. Acad. Sci.* **2009**, *106* (27), 10949–10954.
- (4) Hayman, G. D.; Derwent, R. G. *Environ. Sci. Technol.* **1997**, *31*, 327–336.
- (5) World Petrochemicals - SRI Consulting <http://www.sriconsulting.com/WP/Public/Reports/ipa>.
- (6) Laity, J. L.; Burstain, I. G.; Appel, B. R. *Solvents Theory and Practice, Advances in Chemistry*; American Chemical Society: Washington, DC, 1973; Vol. 124, pp. 95–112.
- (7) Lloyd, A. C.; Darnall, K. R.; Winer, A. M.; Pitts, J. N., Jr. *Chem. Phys. Lett.* **1976**, *42*, 205–209.
- (8) Overend, R.; Paraskevopoulos, G. J. *Phys. Chem.* **1978**, *82*, 1329–1333.
- (9) Klopffer, V. W.; Frank, R.; Kohl, E.-G.; Haag, F. *Chem. Z.* **1986**, *110*, 57–62.
- (10) Wallington, T. J.; Kurylo, M. J. *Int. J. Chem. Kinet.* **1987**, *19*, 1015–1023.
- (11) Nelson, L.; Rattigan, O.; Neavyn, R.; Sidebottom, H.; Treacy, J.; Nielsen, O. J. *Int. J. Chem. Kinet.* **1990**, *22*, 1111–1126.
- (12) Dunlop, J. R.; Tully, F. P. *J. Phys. Chem.* **1993**, *97*, 6457–6464.
- (13) Yujing, M.; Mellouki, A. *Chem. Phys. Lett.* **2001**, *333*, 63–68.
- (14) Wu, H.; Mu, Y.; Zhang, X.; Jiang, G. *Int. J. Chem. Kinet.* **2003**, *35*, 81–87.
- (15) Rajakumar, B.; McCabe, D. C.; Talukdar, R. K.; Ravishankara, A. R. *Int. J. Chem. Kinet.* **2010**, *42*, 10–24.
- (16) Sander, S. P.; Abbatt, J.; Barker, J. R.; Burkholder, J. B.; Friedl, R. R.; Golden, D. M.; Huie, R. E.; Kolb, C. E.; Kurylo, M. J.; Moortgat, G. K.; Orkin, V. L.; Wine, P. H. *Chemical Kinetics and Photochemical Data for Use in Atmospheric Studies, Evaluation No. 17*; JPL Publication 10-6; Jet Propulsion Laboratory, California Institute of Technology: Pasadena, CA, 2011; <http://jpldataeval.jpl.nasa.gov>.
- (17) Atkinson, R.; Baulch, D. L.; Cox, R. A.; Crowley, J. N.; Hampson, R. F.; Hynes, R. G.; Jenkin, M. E.; Rossi, M. J.; Troe, J.; Wallington, T. J.; *Atmos. Chem. Phys.* **2006**, *8*, 4141–4496, IUPAC Subcommittee for Gas Kinetic Data Evaluation, <http://www.iupac-kinetic.ch.cam.ac.uk>.
- (18) Tokuhashi, K.; Nagai, H.; Takahashi, A.; Kaise, M.; Kondo, S.; Sekiya, A.; Takahashi, M.; Gotoh, Y.; Suga, A. *J. Phys. Chem. A* **1999**, *103*, 2664–2672.
- (19) Certain commercial equipment, instruments, or materials are identified in this article in order to adequately specify the experimental procedure. Such identification does not imply recognition or endorsement by the National Institute of Standards and Technology, nor does it imply that the material or equipment identified are necessarily the best available for the purpose.
- (20) Kurylo, M. J.; Cornett, K. D.; Murphy, J. L. *J. Geophys. Res.* **1982**, *87*, 3081–3085.
- (21) Orkin, V. L.; Huie, R. E.; Kurylo, M. J. *J. Phys. Chem.* **1996**, *100*, 8907–8912.
- (22) Orkin, V. L.; Khamaganov, V. G.; Guschin, A. G.; Huie, R. E.; Kurylo, M. J. *J. Phys. Chem.* **1997**, *101*, 174–178.
- (23) Orkin, V. L.; Martynova, L. E.; Ilichev, A. N. *J. Phys. Chem.* **2010**, *114*, 5967–5979.
- (24) Orkin, V. L.; Khamaganov, V. G.; Martynova, L. E.; Kurylo, M. J. *J. Phys. Chem.* **2011**, *115*, 8656–8668.
- (25) Kurylo, M. J.; Orkin, V. L. *Chem. Rev.* **2003**, *103*, 5049–5076.
- (26) Spivakovskiy, C. M.; Logan, J. A.; Montzka, S. A.; Balkanski, Y. J.; Foreman-Fowler, M.; Jones, D. B. A.; Horowitz, L. W.; Fusco, A. C.; Brenninkmeijer, C. A. M.; Prather, M. J.; Wofsy, S. C.; McElroy, M. B. *J. Geophys. Res.* **2000**, *105*, 8931–8980 and references contained therein.
- (27) Hess, W. P.; Tully, F. P. *Chem. Phys. Lett.* **1988**, *152*, 183–189.
- (28) Carr, S.; Shallcross, D. E.; Canosa-Mas, C.; Wenger, J. C.; Sidebottom, H. W.; Treacy, J. J.; Wayne, R. P. *Phys. Chem. Chem. Phys.* **2003**, *5*, 3874–3883.
- (29) Kozlov, S. N.; Orkin, V. L.; Huie, R. E.; Kurylo, M. J. *J. Phys. Chem. A* **2003**, *107*, 1333–1338.
- (30) Kozlov, S. N.; Orkin, V. L.; Kurylo, M. J. *J. Phys. Chem. A* **2003**, *107*, 2239–2246.
- (31) Orkin, V. L.; Kozlov, S. N.; Poskrebyshev, G. A.; Kurylo, M. J. *J. Phys. Chem. A* **2006**, *110*, 6978–6985.
- (32) Meier, U.; Grotheer, H.-H.; Riekert, G.; Just, Th. *Chem. Phys. Lett.* **1985**, *133*, 221–225.
- (33) Wang, Y.; Liu, J. Y.; Li, Z. S.; Wang, L.; Sun, C. C. *J. Comput. Chem.* **2007**, *28*, 802–810.

(34) Harrison, A. J.; Cederholm, B. J.; Terwilliger, M. A. *J. Chem. Phys.* **1959**, *30*, 355–356.

(35) Salahub, D. R.; Sandorfy, C. *Chem. Phys. Lett.* **1971**, *8*, 71–74.

(36) Keller-Rudek, H.; Moortgat, G. K., MPI-Mainz-UV-VIS Spectral Atlas of Gaseous Molecules; www.atmosphere.mpg.de/spectral-atlas-mainz

(37) Prinn, R. G.; Huang, J.; Weiss, R. F.; Cunnold, D. M.; Fraser, P. J.; Simmonds, P. G.; McCulloch, A.; Harth, C.; Salameh, P.; O'Doherty, S.; Wang, R. H. J.; Porter, L.; Miller, B. R. *Science* **2001**, *292*, 1882.

(38) Orkin, V. L.; Khamaganov, V. G.; Guschin, A. G.; Kasimovskaya, E. E.; Larin, I. K. *Development of Atmospheric Characteristics of Chlorine-Free Alternative Fluorocarbons*. Report on R-134a and E-143a, Report ORNL/Sub/86X-SL103V prepared for the Oak Ridge National Laboratory, 1993.

(39) Orkin, V. L.; Guschin, A. G.; Larin, I. K.; Huie, R. E.; Kurylo, M. J. *J. Photochem. Photobiol. A* **2003**, *157*, 211–222.